

# Statistical Damage Classification Using Sequential Probability Ratio Tests

Hoon Sohn,<sup>1,\*</sup> David W. Allen,<sup>1</sup> Keith Worden<sup>2</sup> and Charles R. Farrar<sup>1</sup>

<sup>1</sup>*Engineering Sciences and Applications Division, Weapon Response Group, M/S T006, Los Alamos National Laboratory, Los Alamos, NM 87545, USA*

<sup>2</sup>*Department of Mechanical Engineering, University of Sheffield, Mappin Street, Sheffield S1 3JD, UK*

The primary objective of damage detection is to ascertain with confidence if damage is present or not within a structure of interest. In this study, a damage classification problem is cast in the context of the statistical pattern recognition paradigm. First, a time prediction model, called an autoregressive and autoregressive with exogenous inputs (AR-ARX) model, is fit to a vibration signal measured during a normal operating condition of the structure. When a new time signal is recorded from an unknown state of the system, the prediction errors are computed for the new data set using the time prediction model. When the structure undergoes structural degradation, it is expected that the prediction errors will increase for the damage case. Based on this premise, a damage classifier is constructed using a sequential hypothesis testing technique called the sequential probability ratio test (SPRT). The SPRT is one form of parametric statistical inference tests, and the adoption of the SPRT to damage detection problems can improve the early identification of conditions that could lead to performance degradation and safety concerns. The sequential test assumes a probability distribution of the sample data sets, and a Gaussian distribution of the sample data sets is often used. This assumption, however, might impose potentially misleading behavior on the extreme values of the data, i.e. those points in the tails of the distribution. As the problem of damage detection specifically focuses attention on the tails, the assumption of normality is likely to lead the analysis astray. To overcome this difficulty, the performance of the SPRT is improved by integrating extreme values statistics, which specifically models behavior in the tails of the distribution of interest into the SPRT.

**Keywords** damage detection · time series analysis · sequential probability ratio test · extreme value statistics · statistical pattern recognition · vibration test

## 1 Introduction

The most primary goal of structural health monitoring and damage detection is simply to identify from measured data if a structure of engineering interest has deviated from a normal operational condition. In particular, vibration-based damage detection techniques assume that changes of

the structure's integrity affect characteristics of the measured vibration signals enabling one to detect damage. The area of structural health monitoring that receives the most attention in the technical literature is feature extraction (Doebeling et al., 1998). Feature extraction is the process of identifying damage-sensitive properties, derived

\*Author to whom correspondence should be addressed.  
E-mail: [sohn@lanl.gov](mailto:sohn@lanl.gov)

from the measured vibration response, which allows one to distinguish between the undamaged and damaged states of the structure. On the other hand, the least attention is paid to the development of statistical inference tools to enhance the actual damage classification process. A statistical inference is concerned with the implementation of the algorithms that operate on the extracted features to quantify the damage state of the structure.

In this paper, a unique combination of time series analysis, statistical pattern recognition techniques, and extreme value statistics is presented to automate the damage identification procedure with special attention to statistical inference for decision-making. The structure of this paper is as follows. Section 2 briefly reviews the time series analysis of vibration signals using the autoregressive and autoregressive with exogenous inputs (AR-ARX) model. Section 3 outlines the main theory of the sequential probability ratio test (SPRT), and Section 4 incorporates extreme value statistics to the SPRT. The SPRT is applied to numerical and experimental data in Sections 5 and 6, respectively. Section 7 concludes and summarizes the findings of this study.

## 2 Time Series Analysis

The time series analysis begins with the assumption that a “pool” of signals is acquired from a system with a known structural condition. In the experimental example reported later on, multiple time series are recorded from the undamaged structure. The collection of these time series is called the “reference database” in this study. The construction of this reference database is shown to be useful for normalizing data with respect to varying operational and environmental conditions. The applications of this time series analysis to data normalization are presented in Sohn and Farrar (2001) and Sohn et al. (2001).

A linear prediction model combining autoregressive (AR) and autoregressive with exogenous inputs (ARX) models is employed to compute the damage-sensitive feature. In this case, the damage-sensitive feature is the standard deviation of the residual error between the prediction model and measured time series.

First, all time signals are standardized prior to fitting an AR model such that;

$$\hat{x} = \frac{x - \mu_x}{\sigma_x} \quad (1)$$

where  $\hat{x}$  is the standardized signal,  $\mu_x$  and  $\sigma_x$  are the mean and standard deviation of  $x$ , respectively. This standardization procedure is applied to all signals employed in this study. However, for simplicity,  $x$  is used to denote  $\hat{x}$  hereafter.

For each time series  $x(t)$  in the reference database, an AR model with  $r$  autoregressive terms is constructed. An AR( $r$ ) model can be written as (Box et al., 1994):

$$x(t) = \sum_{j=1}^r \phi_{xj} x(t-j) + e_x(t) \quad (2)$$

This step is repeated for all signals in the reference database.

Employing a new segment  $y(t)$  obtained from an unknown structural condition of the system, repeat the previous step. Here the new segment  $y(t)$  has the same length as the signal  $x(t)$ :

$$y(t) = \sum_{j=1}^r \phi_{yj} y(t-j) + e_y(t) \quad (3)$$

Then, the signal segment  $x(t)$  “closest” to the new signal block  $y(t)$  is defined as the one that minimizes the following difference of AR coefficients:

$$\text{Difference} = \sum_{j=1}^r (\phi_{xj} - \phi_{yj})^2 \quad (4)$$

This “data normalization” is a procedure to select the previously recorded time signal from the reference database, which is recorded under operational and/or environmental conditions closest to that of the newly obtained signal. If the new signal block is obtained from an operational condition close to one of the reference signal segments and there has been no structural deterioration or damage to the system, the dynamic characteristics (in this case, the AR coefficients) of the new signal should be similar

or close to those of the reference signal based on the Euclidean distance measure in Equation (4).

When a time prediction model is constructed from the selected reference signal, this prediction model should be able to appropriately predict the new signal if the new signal is “close” to the reference signal. On the other hand, if the new signal were recorded under a structural condition different from the conditions where the reference signal was obtained, the prediction model estimated from even the “closest” signal in the reference database would not reproduce the new signal well.

The prediction capability of an AR model can be examined by computing the standard deviation of the prediction error  $e_x(t)$ . If the dynamic characteristics of a time series  $x(t)$  can be well represented by the AR model, the standard deviation of the associated prediction error  $e_x(t)$  should be relatively small. In fact, it is recommended to keep the standard deviation of the prediction errors less than 10% of the standard deviation of the original signal  $x(t)$ . This condition implies that the AR model is able to capture more than 90% of the underlying dynamics of the system, and the prediction error makes up the remaining uncertainties of the signal dynamics. For the experimental study presented later, it turns out that the standard deviation of the prediction error ranges around 30–40% of the standard deviation of the original time signal indicating that the AR model is not capable of predicting the time signal properly.

To overcome this problem, a two-step prediction model called AR-ARX model is employed in this study. Other applications of this AR-ARX model are presented in Sohn and Farrar (2001) and Sohn et al. (2001). For the construction of a two-stage prediction model, it is assumed that the error between the measurement and the prediction obtained by the AR model [ $e_x(t)$  in Equation (2)] is mainly caused by an unknown external input. Based on this assumption, an ARX model is employed to reconstruct the input/output relationship between  $e_x(t)$  and  $x(t)$ ;

$$x(t) = \sum_{i=1}^p \alpha_i x(t-i) + \sum_{j=1}^q \beta_j e_x(t-j) + \varepsilon_x(t) \quad (5)$$

where  $\varepsilon_x(t)$  is the residual error after fitting the ARX( $p, q$ ) model to  $e_x(t)$  and  $x(t)$  pair. The feature for damage diagnosis will later be related to this quantity  $\varepsilon_x(t)$ . Note that this AR-ARX modeling is similar to a linear approximation method of an autoregressive moving-average (ARMA) model presented in Ljung (1987) and references therein. Ljung (1987) suggested keeping the sum of  $p$  and  $q$  smaller than  $r$  ( $p + q \leq r$ ). Although the  $p$  and  $q$  values of the ARX model are set rather arbitrarily, similar results are obtained for different combinations of  $p$  and  $q$  values as long as the sum of  $p$  and  $q$  is kept smaller than  $r$ .

Next, it is investigated how well this ARX( $p, q$ ) model estimated in Equation (5) reproduces the input/output relationship of  $e_y(t)$  and  $y(t)$ ;

$$\varepsilon_y(t) = y(t) - \sum_{i=1}^p \alpha_i y(t-i) - \sum_{j=1}^q \beta_j e_y(t-j) \quad (6)$$

where  $e_y(t)$  is considered to be an approximation of the system input estimated from Equation (3). Note that the  $\alpha_i$  and  $\beta_j$  coefficients are associated with  $x(t)$  and obtained from Equation (5). If the ARX model obtained from the reference signal block  $x(t)$  and  $e_x(t)$  pair were not a good representative of the newly obtained signal segment  $y(t)$  and  $e_y(t)$  pair, there would be a significant change in the standard deviation of the residual error  $\varepsilon_y(t)$  compared to that of  $\varepsilon_x(t)$ . Therefore, the standard deviation of the residual error is defined as the damage-sensitive feature and the increase of this standard deviation is monitored using the following SPRT.

### 3 Damage Classification Using Sequential Probability Ratio Tests

The SPRT procedure is particularly relevant if the data are collected sequentially (Wald, 1947). Examples of such sequential collection include failures on a production line, patient throughput in a hospital or relapses in behavioral interventions. Sequential analysis is different from classical hypothesis testing where the number of samples tested or collected is fixed at the beginning of the

experiment. In classical hypothesis testing the data collection is executed without analysis and consideration of the data. After all data are collected, the analysis is done and conclusions are drawn. However, in sequential analysis every data point is analyzed directly after being collected, the data collected up to that moment are then compared with threshold values, incorporating the new information obtained from the freshly collected case. This approach allows one to draw conclusions during the data collection, and a final conclusion can possibly be reached at a much earlier stage than in the case of classical hypothesis testing. The advantages of sequential analysis are easy to see. As data collection can be terminated after fewer samples and decisions drawn earlier, the savings in terms of human life and misery, and financial savings might be considerable. Particularly, the framework of this sequential analysis suits the paradigm of continuous structural health monitoring very well.

### 3.1 Sequential Test

A sequential statistical inference starts with the accumulation of a sequence of random variables  $\{x_i\}(i = 1, 2, \dots)$ . This accumulated data set at stage  $n$  is denoted as:

$$X_n = (x_1, \dots, x_n) \quad (7)$$

For the experimental study presented later, this accumulated data set will be a collection of the residual errors computed from the AR-ARX model presented in the previous section. The goal of a statistical inference is to reveal the probability model of  $X_n$ , which is assumed to be at least partially unknown. When the statistical inference is cast as a parametric problem, the functional form of  $X_n$  is assumed to be known and the statistical inference poses some questions regarding the parameters of the probability model. For instance, if  $\{x_i\}$  are independent and identically distributed (i.i.d) normal variables, one may pose some statistical test about the mean and/or the variance of this normal distribution.

A sequential test is one of the simplest tests for such a statistical inference where the number of samples required before reaching a decision is

not determined in advance. An advantage of the sequential test is that on an average a smaller number of observations is needed to make a decision compared to the conventional fixed-sample size test. First, a simple hypothesis test containing only two distinct distributions is considered. Here, the interest is in discriminating two simple hypotheses;

$$H_0 : \theta = \theta_0, \quad H_1 : \theta = \theta_1, \quad \theta_0 \neq \theta_1 \quad (8)$$

where  $\theta$  is a particular parameter value in question, and it is assumed that  $\theta$  can take either  $\theta_0$  or  $\theta_1$  only. In general,  $\theta$  can be a vector of multiple parameters. However,  $\theta$  is assumed to be a single parameter for the sake of simplicity in this study. When a sequence of observations  $\{x_i\}$  is available, the purposes of any sequential test for the above hypotheses are (1) to reach the correct decision about  $H_0$  with the least probability of Type I and II errors, (2) to minimize the sampling number before the correct decision is made, and (3) to eventually terminate with either the acceptance or rejection of  $H_0$  as the sampling size  $n$  increases. Here, Type I error arises if  $H_0$  is rejected when in fact it is true. Type II error arises if  $H_0$  is accepted when it is false. When a sequential test satisfies the last condition, the test is defined closed. Otherwise, an open test may continue infinitely observing data without reaching any terminal decision about  $H_0$ .

It turns out that the simultaneous achievement of all three goals is impossible by any tests. Therefore, a reasonable compromise among these conflicting goals needs to be achieved. For the well-established fixed-sampling test, the sample size  $n$  is fixed, and an upper bound on the Type I error is prespecified. Then, an optimal fixed-sample test is selected by minimizing the probability of Type II error. On the other hand, a sequential test specifies upper bounds on the probabilities of Type I and II errors and minimizes the following average sample number,  $E(n|\theta)$ ;

$$E(n|\theta) = \sum_{n=1}^{\infty} nP(n|\theta) \quad (9)$$

where  $P(n|\theta)$  is the probability mass function of  $n$  when  $\theta$  is the true value of the parameter. That is, a sequential test attempts to minimize the sample number needed to make a decision in an average sense. Note that, when a sequential test is closed,  $P(n < \infty|\theta) = 1$  for  $\theta = \theta_o$  or  $\theta_1$ . This means that any closed sequential test will be eventually terminated as the sample size increases.

There exists a class of valid sequential tests, which satisfy the following criteria (Ghosh, 1970):

- (1) the test is closed;
- (2)  $1 - Q(\theta) \leq \alpha$ , for  $\theta = \theta_o$ ;
- (3)  $Q(\theta) \leq \beta$ , for  $\theta = \theta_1$ .

where  $\alpha$  and  $\beta$  are the preassigned Type I and II errors, respectively.  $Q(\theta)$  is the probability that any sequential test accepts  $H_o$  as  $n \rightarrow \infty$ . In other words,

$$Q(\theta) = \sum_{n=1}^{\infty} \int_{X_n \in R_o^n} f(X_n|\theta) dX_n \quad (11)$$

where  $f(X_n|\theta)$  is the conditional probability density function of observing the accumulated data set  $X_n$  given the assumption of  $\theta$ . The integral in Equation (11) is evaluated over the acceptance region of  $H_o$  ( $X_n \in R_o^n$ ). The second criterion in Equation (10) states that for all values of  $n$ , the true Type I error,  $1 - Q(\theta_o)$ , should be less than the preassigned risk  $\alpha$ . In a similar fashion, the third criterion indicates that the true Type II error  $Q(\theta_1)$  should be less than  $\beta$ .

Among various valid sequential tests, it can be analytically proven that the SPRT minimizes the average sample number required to make a correction rendering this test an optimal sequential test (Ghosh, 1970). Because of this extreme sensitivity of the SPRT to signal disturbance, the SPRT has been applied for the surveillance of nuclear power plant components (Humenik and Gross, 1990; Gross and Humenik, 1991).

When implementing the SPRT, a trade-off must be considered before assigning values for  $\alpha$  and  $\beta$ . When there is a large penalty associated with false positive alarms (for example, alarms that shut down traffic over a bridge), it is

desirable to keep  $\alpha$  smaller than  $\beta$ . On the other hand, for the safety of critical systems such as nuclear power plants, one might be more willing to tolerate a false positive alarm to have a higher degree of safety assurance. In this case, it is not uncommon to specify  $\beta$  larger than  $\alpha$ .

### 3.2 Sequential Probability Ratio Test

Using a SPRT,  $S(b, a)$ , the hypothesis test stated in Equation (8) is reformulated as follows (Ghosh, 1970);

Record a sequence of observations  $\{x_i\}$  ( $i = 1, 2, \dots$ ) successively, and at stage  $n$ :

- (1) accept  $H_o$ , if  $Z_n \leq b$ ;
- (2) reject  $H_o$ , if  $Z_n \geq a$ ;
- (3) continue observing data, if  $b \leq Z_n \leq a$ .

where the transformed random variable  $Z_n$  is the natural logarithm of the probability ratio at stage  $n$  (it should be clear by now why this test is called a sequential probability ratio test):

$$Z_n = \ln \frac{f(X_n|\theta_1)}{f(X_n|\theta_o)} \quad \text{for } n \geq 1 \quad (13)$$

Without any loss of generality,  $Z_n$  is defined zero when  $f(X_n|\theta_1) = f(X_n|\theta_o) = 0$ .  $b$  and  $a$  are the two stopping bounds for accepting and rejecting  $H_o$ , respectively, and they can be estimated by the following Wald approximations (Wald, 1947):

$$b \cong \ln \frac{\beta}{1 - \alpha} \quad \text{and} \quad a \cong \ln \frac{1 - \beta}{\alpha} \quad (14)$$

Although closed form solutions of  $a$  and  $b$  are available for several probability models, it has been a standard practice to employ Equation (14) to approximate the stopping bounds in all practical applications. The continuation region  $b \leq Z_n \leq a$  is called the critical inequality of  $S(b, a)$  at stage  $n$ .

In many practical problems, it is often more realistic to formulate the hypothesis test as discrimination between two one-sided hypotheses:

$$H_o : \theta \leq \theta_o, \quad H_1 : \theta \geq \theta_1, \quad \theta_o < \theta_1 \quad (15)$$

The criteria in Equation (10) are now equivalent to:

- (1) the test is closed;
- (2)  $1 - Q(\theta) \leq \alpha$ , for  $\theta \leq \theta_o$ ;
- (3)  $Q(\theta) \leq \beta$ , for  $\theta \geq \theta_1$ .

(16)

Ghosh (1970) shows that the previous SPRT shown in Equation (12) also provides an optimal solution to this hypothesis test defined in Equation (15).

### 3.3 Application to Normal Distributions

In the damage detection problem presented, the main interest is to examine how the probability distribution function of the residual errors broadens as data are recorded under a damaged condition of a system. Therefore, the following hypothesis test is constructed using the standard deviation of the residual error as the parameter in question:

$$H_o : \sigma \leq \sigma_o, \quad H_1 : \sigma \geq \sigma_1, \quad 0 < \sigma_o < \sigma_1 \quad (17)$$

Here, when the standard deviation of the residual errors,  $\sigma$ , is equal to or less than a user specified standard deviation value  $\sigma_o$ , the system in question is considered undamaged. On the other hand, when  $\sigma$  becomes equal to or larger than the other user specified standard deviation  $\sigma_1$ , the system is suspected to be damaged. It should be noted that the selection of  $\sigma_o$  and  $\sigma_1$  is structure-dependent, and it might be necessary to use training data sets to establish these two decision boundaries. Obviously, the more data become available for training, the better diagnosis results are obtained. However, there is no minimum training size requirement for the SPRT. One can even assign initial values of  $\sigma_o$  and  $\sigma_1$  based on engineering judgments and experiences, and subsequently adjust these values as more data becomes available. Alternatively, the probability density function (PDF) of the extracted feature can be first approximated using either parameter or nonparametric estimation techniques, and the  $\sigma_o$  and  $\sigma_1$  values associated with a certain confidence interval can be assigned.

If modified observations  $\{z_i\} (i = 1, 2, \dots)$  are defined as follows;

$$z_1 = \ln \frac{f(X_1|\sigma_1)}{f(X_1|\sigma_o)} \quad \text{and} \quad z_i = \ln \frac{f(X_i|\sigma_1)f(X_{i-1}|\sigma_o)}{f(X_i|\sigma_o)f(X_{i-1}|\sigma_1)} \quad (18)$$

then,  $Z_n$  becomes:

$$Z_n = \sum_{i=1}^n z_i \quad (19)$$

Assuming that  $X_n$  has a normal distribution with mean  $\mu$  and standard deviation  $\sigma$ ,  $z_i$  can be related to  $x_i$ :

$$z_i = \frac{1}{2}(\sigma_o^{-2} - \sigma_1^{-2})(x_i - \mu)^2 - \ln \frac{\sigma_1}{\sigma_o} \quad (20)$$

In a graphical representation of a SPRT  $S(b, a)$ ,  $Z_n$ , which is the cumulative sum of the transformed variable  $z_i$ , is continuously plotted against the two stopping bounds  $b$  and  $a$ . It should be noted that the mean  $\mu$  of the distribution is assumed to be known. Even when  $\mu$  is unknown, the aforementioned procedure is still valid if  $x_i$  is replaced by  $y_i$ :

$$y_i = \left( \sum_{j=1}^i x_j - ix_{i+1} \right) / \sqrt{i(i+1)} \quad \text{for } i = 1, 2, \dots \quad (21)$$

It can be shown that now  $\{y_i\}$  has i.i.d normal distribution with zero mean and the same standard deviation as  $\{x_i\}$ .

## 4 Extreme Value Statistics

In the previous section, the SPRT procedure is formulated assuming that the sampled data have a normal distribution. However, the assumption of normality might impose potentially misleading behavior on the extreme values of the data, namely, those points in the tails of the distribution. An alternative approach can be based on extreme value statistics. This branch of statistics

was developed to specifically model behavior in the tails of the distribution of interest.

In fact, there is a large body of statistical theory that is explicitly concerned with modeling the tails of distributions, and these statistical procedures are applied to the current problem of damage classification. The relevant field is referred to as extreme value statistics, a branch of order statistics. There are many excellent textbooks and monographs in this field. Some are considered classics (Gumbel, 1958; Galambos, 1978), and others are more recent (Embrechts et al., 1997; Kotz and Nadarajah, 2000). Castillo (1987) is notable in its concern with engineering problems in fields like meteorology, hydrology, ocean engineering, pollution studies, strength of materials, etc. Although extreme value statistics has been widely applied, there has been little application of these techniques to damage detection.

The major problems with modeling the normal condition of a system are that the functional form of the distribution is unknown and that there are an infinite number of candidate distributions that may be appropriate for the prediction applications. The researcher must choose among various distributions and then estimate parameters based on training data. This process is largely subjective. If extreme value statistics is applied to the tails instead of working with the central statistics of a distribution, there are only three candidate distributions for the tails and the problem of model selection and parameter estimation becomes more objective.

Suppose that one is given a vector of samples  $(x_1, \dots, x_m)$  from an arbitrary parent distribution. The most relevant statistic for studying the tails of the parent distribution is the maximum operator,  $\max(x_1, \dots, x_m)$ , which selects the point of the maximum value from the sample vector. Note that this statistic is relevant for the right tail of a univariate distribution only. For the left tail, the minimum should be used. The pivotal theorem of extreme value statistics (Fisher and Tippett, 1928) states that in the limit as the number of vector samples tends to infinity, the induced distribution on the maxima of the samples can only take one of three forms: Gumbel, Weibull, or Frechet. The rest of this section will be concerned with elaborating on this fact.

If the values of the sequence  $(x_1, \dots, x_m)$  are arranged in ascending order, the  $r$ th element of this sequence  $x_r$  is called the  $r$ th order statistic. The basic question, which now arises is, what are the distributions of the order statistics, in particular, the minimum,  $x_1$ , and the maximum,  $x_m$ .

Following Castillo (1987), let  $n_m(x)$  be the number of samples for which  $x_j \leq x$ . Each time one chooses a value  $x_j$  from the sample, one is conducting a Bernoulli experiment, an experiment that has one of two outcomes, with a probability  $F(x)$ , the cumulative distribution function (CDF), that  $x_j \leq x$ , and the complementary probability,  $1 - F(x)$ , that  $x_j > x$ . The CDF of  $n_m(x)$  is, therefore, a binomial distribution with  $F^k(x)$  denoting the probability of success:

$$F_{n_m(x)}(r) = P(n_m(x) \leq r) = \sum_{k=0}^r \binom{m}{k} F^k(x) [1 - F(x)]^{m-k} \quad (22)$$

Now, because the event  $(x_r \leq x)$  is basically the same as the event  $(n_m(x) \geq r)$ ,  $P(x_r \leq x)$  is identical to  $P(n_m(x) \geq r) = 1 - P(n_m(x) < r)$ . In addition, it follows that  $F_{x_r}(x) = 1 - F_{n_m(x)}(r - 1)$  or

$$F_{x_r}(x) = P(x_r \leq x) = \sum_{k=r}^m \binom{m}{k} F^k(x) [1 - F(x)]^{m-k} \quad (23)$$

If one is concerned with the maximum of the sample, the relevant order statistic is  $x_m$  and the relevant distribution is:

$$F_{x_m}(x) = F^m(x) \quad (24)$$

Concentrating now on the maximum, let  $m \rightarrow \infty$ . Then, the limit distribution for the maximum will satisfy:

$$\lim_{m \rightarrow \infty} F^m(x) = \begin{cases} 1 & \text{If } F(x) = 1 \\ 0 & \text{If } F(x) < 1 \end{cases} \quad (25)$$

This distribution does not make sense because a CDF is developed on the assumption that it is continuous, but here the limit is discontinuous. The way around this discontinuity is to normalize

the independent variable with a sequence of constants ( $x \rightarrow a_m + b_m x$ ) in such a way that;

$$\lim_{m \rightarrow \infty} F^m(a_m + b_m x) = F_M(x) \quad (26)$$

where  $F_M(x)$  is a nondegenerate limit function. In fact, it is required that  $F_M(x)$  be continuous.

Fisher and Tippett (1928) state that, in the limit as the number of vector samples tends to infinity, the induced distribution  $F_M(x)$  in Equation (26) can only take one of the following three forms;

$$\text{Frechet: } F_M(x) = \begin{cases} \exp\left[-\left(\frac{\delta}{x-\lambda}\right)^\beta\right] & \text{if } x \geq \lambda \\ 0 & \text{otherwise} \end{cases} \quad (27)$$

$$\text{Weibul: } F_M(x) = \begin{cases} 1 & \text{if } x \geq \lambda \\ \exp\left[-\left(\frac{\lambda-x}{\delta}\right)^\beta\right] & \text{otherwise} \end{cases} \quad (28)$$

Gumbel:

$$F_M(x) = \exp\left[-\exp\left(-\frac{x-\lambda}{\delta}\right)\right] \quad \begin{matrix} -\infty < x < \infty \\ \delta > 0 \end{matrix} \quad (29)$$

where  $\lambda$ ,  $\delta$ , and  $\beta$  are the model parameters, which should be estimated from the data, and “exp” is an exponential operator.  $F_M(x)$  is, in fact, a cumulative density function (CDF) of maxima and the subscript “ $M$ ” is used to denote that the distribution is for the maxima. Note that these distributions are relevant for the right tail of a univariate distribution only. For the left tail, similar distributions for the minimum can be obtained.

Now given samples of maximum data from a parent population, it is possible to select an appropriate limit distribution and fit a parametric model to the data. It is also possible to fit models to portions of the parent distribution's tails as these models are equivalent in the tail to the appropriate extreme value distribution. Once the appropriate model is obtained, the SPRT can

be reformulated using the known distribution type of the extreme values. In this paper, the discussion is limited to the Gumbel distribution for maxima but similar derivations can be developed for the other extreme distributions.

#### 4.1 A Sequential Probability Ratio Test using a Gumbel Distribution for Maxima

Now, the SPRT is extended to the extreme values of the parent distribution, i.e., the distribution of the residual error. In the previous section, the SPRT is formulated assuming that the residual error has a normal distribution. However, slight deviation from the normality assumption of the parent distribution might lead to larger errors for the extremes resulting in erroneous false positive/negative indications of damage. To avoid this problem, the SPRT is reformulated using the probability distribution of extreme values. Because the maxima of a normal distribution are known to have a Gumbel distribution and the residual error distribution of the experimental study presented later is close to a normal distribution, the derivation presented here focuses on incorporating a Gumbel distribution for maxima values into the SPRT. Similar formulations can be easily derived for other types of extreme value distributions and for minima values.

Similar to Equation (17), the following hypothesis test is constructed using the standard deviation of the maxima as the parameter in question:

$$\begin{aligned} H_0 : \sigma_M \leq \sigma_{M,o}, \quad H_1 : \sigma_M \geq \sigma_{M,1}, \\ 0 < \sigma_{M,o} < \sigma_{M,1} \end{aligned} \quad (30)$$

Now,  $\sigma_M$  is the standard deviation of the residual error maxima, and the subscript “ $M$ ” denotes a quantity related to the maxima.  $\sigma_{M,o}$  is a user specified lower limit of the standard deviation for the undamaged condition, and  $\sigma_{M,1}$  is the other user specified upper limit for the damaged condition. It is observed that the change of the maxima distribution's standard deviation is monotonically related to the change of the parent distribution's standard deviation. Therefore, an indirect statistical inference on the standard deviation of the



parent distribution (the distribution of the residual errors) is conducted by examining the standard deviation of the maximum values.

It can be shown that the model parameters,  $\lambda$  and  $\delta$ , of the Gumble distribution are related to its mean  $\mu_M$  and standard deviation  $\sigma_M$  (Castillo, 1987):

$$\delta = \frac{\sqrt{6}}{\pi} \sigma_M \quad \text{and} \quad \lambda = \mu_M - 0.57772\delta \quad (31)$$

If the distribution of the maxima is preprocessed such that the mean value is zero, Equation (18) can be rewritten in terms of  $\lambda$  and  $\delta$ :

$$z_1 = \ln \frac{f_M(X_1|\lambda_1, \delta_1)}{f_M(X_1|\lambda_o, \delta_o)} \quad (32)$$

$$\text{and } z_i = \ln \frac{f_M(X_i|\lambda_1, \delta_1)f_M(X_{i-1}|\lambda_o, \delta_o)}{f_M(X_i|\lambda_o, \delta_o)f_M(X_{i-1}|\lambda_1, \delta_1)}$$

where  $\lambda_o$  and  $\delta_o$  are parameters related to the null hypothesis  $H_o$ , and  $\lambda_1$  and  $\delta_1$  correspond to the alternative hypothesis  $H_1$ . Again, the subscript “ $M$ ” denotes a quantity related to the maxima. For the original SPRT,  $X_n$  is defined as the accumulated sample points up to stage  $n$  [see Equation (7)]. When the SPRT is applied to the maximum values like in Equation (32),  $X_n = (x_1, \dots, x_n)$  becomes a collection of the maximum values instead. That is,  $x_i$  in  $X_n$  now becomes a maximum value obtained from a sample size of  $m$ . If  $\{x_i\}$  are i.i.d,  $f_M(X_i|\lambda_1, \delta_1)$  becomes  $f_M(x_1|\lambda_1, \delta_1) \times f_M(x_2|\lambda_1, \delta_1) \times \dots \times f_M(x_i|\lambda_1, \delta_1)$  and Equation (32) can be further simplified as follows:

$$z_i = \ln \frac{f_M(x_i|\lambda_1, \delta_1)}{f_M(x_i|\lambda_o, \delta_o)} \quad \text{for } i = 1, 2, \dots, n \quad (33)$$

Next, the PDF of the Gumble distribution for maximum is obtained by differentiating the CDF presented in Equation (29):

$$\begin{aligned} f_M(x) &= \frac{dF_M(x)}{dx} \\ &= \frac{1}{\delta} \exp\left(-\frac{x-\lambda}{\delta}\right) \exp\left[-\exp\left(-\frac{x-\lambda}{\delta}\right)\right] \end{aligned} \quad (34)$$

By substituting Equation (34) into Equation (33),  $z_i$  can be related to  $x_i$ :

$$\begin{aligned} z_i &= -\ln \frac{\delta_1}{\delta_o} + \left(\frac{x_i - \lambda_o}{\delta_o}\right) - \left(\frac{x_i - \lambda_1}{\delta_1}\right) \\ &\quad + \exp\left(-\frac{x_i - \lambda_o}{\delta_o}\right) - \exp\left(-\frac{x_i - \lambda_1}{\delta_1}\right) \end{aligned} \quad (35)$$

By relating  $\lambda$  and  $\sigma$  to  $\sigma_M$  as shown in Equation (31), Equation (35) can be further simplified as follows:

$$\begin{aligned} z_i &= -\ln \frac{\sigma_1}{\sigma_o} + \frac{\pi}{\sqrt{6}}(\sigma_o^{-1} - \sigma_1^{-1})x_i \\ &\quad + \exp\left(-\frac{x_i + 0.4504\sigma_o}{\sqrt{6}\sigma_o/\pi}\right) - \exp\left(-\frac{x_i + 0.4504\sigma_1}{\sqrt{6}\sigma_1/\pi}\right) \end{aligned} \quad (36)$$

Finally, the cumulative sum of the transformed variable  $Z_i$  is monitored against the two stopping bounds,  $a$  and  $b$ .

#### 4.2 A SPRT using Extreme Value Statistics with a Known Gaussian Parent Distribution

In this section, the SPRT is modified assuming that the parent distribution of the maxima has a known Gaussian distribution. Equation (24) shows that when the parent distribution has a CDF  $F(x)$ , the CDF for the maxima extracted from a sample size  $m$  becomes  $F^m(x)$ . Then, the CDF and the associated PDF of maxima are obtained;

$$F_M(x) = F^m(x) \quad \text{and} \quad f_M(x) = mF^{m-1}(x)f(x) \quad (37)$$

where  $F_M(x)$  and  $f_M(x)$  are the CDF and PDF of the maxima values, and  $F(x)$  and  $f(x)$  are the CDF and PDF of a normal distribution, respectively. By substituting Equation (37) into Equation (18), the following  $z_i$  statistic is obtained:

$$\begin{aligned}
z_i &= \ln \frac{f_M(x_i|\sigma_1)}{f_M(x_i|\sigma_o)} = \ln \frac{nF^{n-1}(x_i|\sigma_1)f(x_i|\sigma_1)}{nF^{n-1}(x_i|\sigma_o)f(x_i|\sigma_o)} \\
&= \frac{1}{2}(\sigma_o^{-2} - \sigma_1^{-2})(x_i - \mu)^2 - \ln \frac{\sigma_1}{\sigma_o} \\
&\quad + (m-1) \ln \frac{F(x_i|\sigma_1)}{F(x_i|\sigma_o)}
\end{aligned} \quad (38)$$

Note that, when the sampling size for the maxima becomes one ( $m=1$ ), Equation (38) reduces back to Equation (20).

## 5 Numerical Examples

In this section, the performances of three variations of the SPRT are compared for different types of parent distributions. The three variations of the SPRT include (1) the conventional SPRT with the normality assumption of data sets [Equation (20)], (2) a SPRT using a Gumbel distribution for maxima [Equation (36)], and (3) a SPRT using extreme value statistics with a known Gaussian parent distribution [Equation (38)]. Hereafter, these techniques are referred to as SPRT-1, SPRT-2, and SPRT-3, respectively. These three SPRT techniques are applied to data sets generated from Gaussian, lognormal, and Gamma distributions.

For a given distribution type of population, two data sets are randomly generated. The first set of data consists of 8192 data points and has a known standard deviation of  $\sigma_x$ . The second data set also consists of 8192 data points and has a modified standard deviation of  $\sigma_y = F\sigma_x$ . Here,  $F$  is a multiplication factor varying from 0.90 to 1.00, 1.10, 1.15, 1.45, 1.50, 1.60 and 1.70. The first data set simulates the residual errors from the initial intact condition of the structure, and the second data set represents the residual errors from a new structural condition of the structure.

The damage classification problem is cast in such a way that, if the standard deviation of the new signal  $\sigma_y$  becomes above a predetermined upper limit  $1.4\sigma_x$ , then the new signal is considered from a damaged state of the system. On the other hand, if  $\sigma_y$  is less than the other predetermined lower limit  $1.2\sigma_x$ , the new signal is then assumed to be from the undamaged condition.

Otherwise (when  $1.2\sigma_x < \sigma_y < 1.4\sigma_x$ ), the damage classifier cannot make a confident decision regarding the current state of the structure and continues collecting additional data. In the numerical examples, the upper and lower limits,  $1.2\sigma_x$  and  $1.4\sigma_x$ , are selected rather arbitrarily. In real applications, the sensitivity of the residual errors with respect to damage of interest might be first examined to establish these two limits. This sequential hypothesis test can be stated in a simplified format:

$$H_o : \sigma_y \leq 1.2\sigma_x \quad \text{and} \quad H_1 : \sigma_y \geq 1.4\sigma_x \quad (39)$$

Because the statistical inference in Equation (39) is imposed only on the unknown standard deviation  $\sigma_y$ , it is assumed that the mean of the signals is zero. Therefore, the mean of each signal is subtracted from the signal.

When the SPRT is combined with maximum value statistics (SPRT-2 and SPRT-3), a moving window of 16 time samples is stepped through the 8192 points of each data set to generate 512 maxima for each condition. That is, the sample size for the maximum value selection is set to be 16 ( $m=16$ ). For all numerical examples, the upper bounds of Type I and II errors are set to 0.001. The corresponding two bounds are  $b=-6.9$  and  $a=6.9$ , respectively. It should be noted that because the parent distribution is assumed unknown for SPRT-2, the hypothesis test in Equation (39) cannot be performed and an alternative hypothesis test is conducted on the standard deviation of the “maximum” values;

$$H_o : \sigma_{M,y} \leq 1.2\sigma_{M,x} \quad \text{and} \quad H_1 : \sigma_{M,y} \geq 1.4\sigma_{M,x} \quad (40)$$

where  $\sigma_{M,x}$  and  $\sigma_{M,y}$  are the standard deviations of the “maximum” values for the first and second sets of signals, respectively.

Three different parent distribution types are investigated in this section: normal, lognormal, gamma distributions. These three distributions are selected because the maxima of all three distributions have Gumbel distributions. In real applications, because the distribution type of the parent data set is unknown, the distribution type of the maximum values should be first chosen.

Because there are only three possible choices for the extreme value statistics, this step is straightforward and is well explained in Castillo (1987).

### 5.1 Gaussian Parent Distribution

In the first example, the parent distribution is assumed normal. Then, the three SPRTs are applied to the numerical data generated from normal distributions. Table 1 summarizes the results of the sequential hypothesis testing. Each entry in Table 1 has three numbers. The first number denotes the number of tests accepting the right hypothesis, and the second number denotes the number of hypothesis tests rejecting the right hypothesis. The last one is the number of cases where the SPRT cannot draw decisions based on the given data sets. For example, when  $F=1.10$ , Table 1 reports that SPRT-2 accepts the right

null hypothesis 63 times out of 100 simulations, and rejects the correct hypothesis 16 times and no decision is made for the remaining 21 cases.

As expected, SPRT-1 and SPRT-3, which are based on the normality assumption of the parent distribution, have accepted the correct hypothesis 100% of time. However, SPRT-2 with the Gumbel distribution of the maxima has several misclassifications near the lower decision boundary (when  $F=1.10$  and 1.15). These misclassifications are mainly caused by the discrepancy between the stated hypothesis test and the actual hypothesis test conducted for SPRT-2. The original hypothesis test is supposed to be performed on the standard deviation of the "parent distribution". However, because the parent distribution type is unknown for SPRT-2, the actual hypothesis test is conducted on the standard deviation of the "extreme distribution". There-

**Table 1** Damage classification results for normal distribution data.

Hypo $F$	$H_0$				$H_1$			
	0.90	1.00	1.10	1.15	1.45	1.50	1.60	1.70
SPRT-1	100/0/0*	100/0/0	100/0/0	100/0/0	100/0/0	100/0/0	100/0/0	100/0/0
SPRT-2	100/0/0	100/0/0	63/16/21	31/47/22	100/0/0	100/0/0	100/0/0	100/0/0
SPRT-3	100/0/0	100/0/0	100/0/0	100/0/0	100/0/0	100/0/0	100/0/0	100/0/0

\*The first number denotes the number of accepting the right hypothesis, and the second number denotes the number of rejecting the correct hypothesis. The last one is the number of cases where the SPRT cannot draw decisions based on the given data sets. For example, 100/0/0 means that, out of 100 simulations, 100 cases are correctly assigned to the true hypothesis and there were no misclassification nor undecided cases.

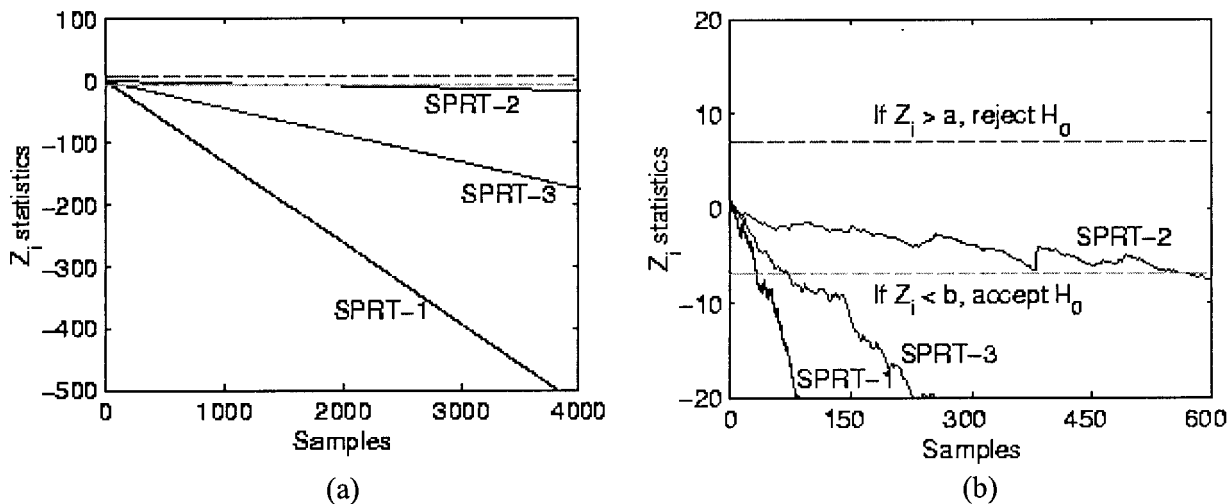


**Figure 1** A typical damage classification result for data sets from a normal distribution, (Correct decision: accepting  $H_0$ ): (a) shown from 1 to 4000 points; (b) shown from 1 to 600 points.

fore, caution should be paid when the classification results in Table 1 are compared for the three different SPRTs.

Figure 1 shows the typical results of the sequential tests. When the  $Z$  statistic goes below the lower bound at  $b = -6.9$ , the null hypothesis is accepted. On the other hand, when the  $Z$  statistic becomes larger than the upper bound  $a = 6.9$ , the null hypothesis is rejected and the alternative hypothesis is accepted. In this particular case shown in Figure 1, accepting the null hypothesis is the correct answer, and all sequential tests make the right classification. It is shown that SPRT-1 generally comes to a decision earlier than the other two sequential tests. Because the extreme values for SPRT-2 and SPRT-3 are sampled at every 16th point from the parent data, it is intuitively expected that the statistical inference using SPRT-1 will come to a conclusion faster than those using SPRT-2 or SPRT-3.

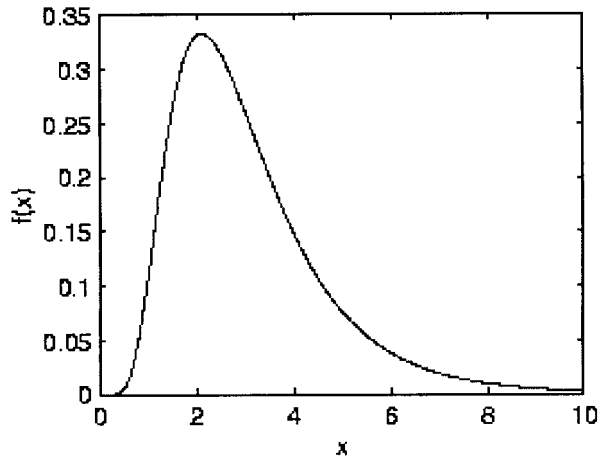


**Figure 2** A lognormal density function with  $\nu = 1.0$  and  $s = 0.5$ .

## 5.2 Lognormal Parent Distribution

In the second numerical example, the parent distribution is assumed lognormal instead of normal. A random variable  $x$  has a lognormal distribution if the natural logarithm of  $x$  is normal (Ang and Tang, 1975). For a lognormal distribution, the PDF of  $x$  becomes;

$$f(x) = \frac{1}{\sqrt{2\pi}sx} \exp \left[ -\frac{1}{2} \left( \frac{\ln x - \nu}{s} \right)^2 \right] \quad (41)$$

where  $\ln x$  is the natural logarithm of  $x$ .  $\nu$  and  $s$  are the mean and standard deviation of  $\ln x$ , respectively. For this simulation,  $\nu = 1.0$  and  $s = 0.5$  are assumed. The associated lognormal density function is displayed in Figure 2. The skewness and kurtosis of this distribution are 1.74 and 8.45, respectively. Note that, for all normal distributions, the values of the skewness and kurtosis should be 0.0 and 3.0, respectively (Wirsching et al., 1995). Therefore, the departure of the skewness and kurtosis values from 0.0 and 3.0 indicates non-Gaussian nature of the data.

The analysis results are summarized in Table 2. Although the formulation of SPRT-1 is based on the normality assumption, SPRT-1 surprisingly performs well even for a lognormal distribution. The performance of SPRT-2 is comparable with the previous result of the normal case. Again, the several misclassifications of SPRT-2 in Table 2 are mainly attributed to the difference between the stated and actual hypothesis tests. SPRT-3 completely misses the true hypothesis when  $F = 1.10$  and 1.15. It seems that the incorrect assumption of the parent distribution produces accumulated errors in the

**Table 2** Damage classification results for lognormal distribution data.

$H_{ypo}$	$H_o$				$H_1$			
	$0.90$	$1.00$	$1.10$	$1.15$	$1.45$	$1.50$	$1.60$	$1.70$
SPRT-1	100/0/0*	100/0/0	100/0/0	99/1/0	100/0/0	100/0/0	100/0/0	100/0/0
SPRT-2	100/0/0	100/0/0	93/1/6	66/15/19	100/0/0	100/0/0	100/0/0	100/0/0
SPRT-3	100/0/0	11/89/0	0/100/0	0/100/0	100/0/0	100/0/0	100/0/0	100/0/0

\*The first number denotes the number of accepting the right hypothesis, and the second number denotes the number of rejecting the correct hypothesis. The last one is the number of cases where the SPRT cannot draw decisions based on the given data sets. For example, 100/0/0 means that, out of 100 simulations, 100 cases are correctly assigned to the true hypothesis and there were no misclassification nor undecided cases.

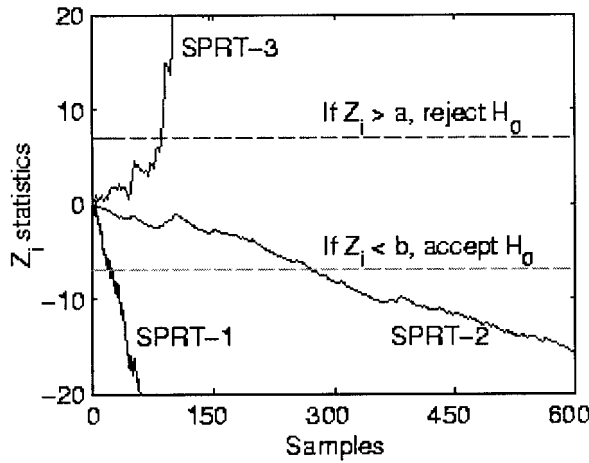


**Figure 3** A typical damage classification result for data sets from a lognormal distribution (Correct decision: accepting  $H_0$ ).

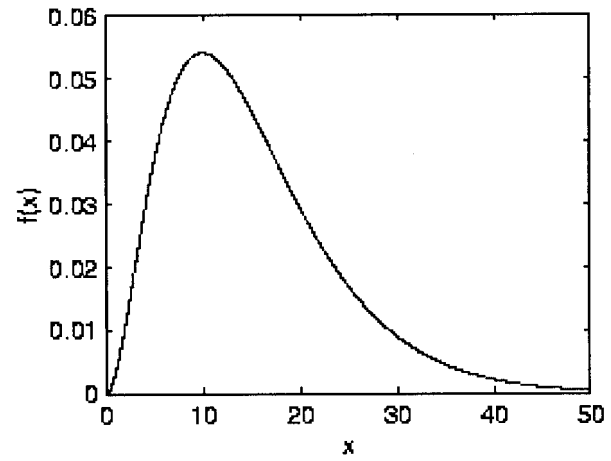


**Figure 4** A gamma density function with  $k=3.0$  and  $\nu=0.2$ .

**Table 3** Damage classification results for gamma distribution data.

Hypo	$H_0$				$H_1$			
	0.90	1.00	1.10	1.15	1.45	1.50	1.60	1.70
SPRT-1	100/0/0*	100/0/0	100/0/0	100/0/0	100/0/0	100/0/0	100/0/0	100/0/0
SPRT-2	100/0/0	100/0/0	99/1/0	83/1/16	98/0/2	100/0/0	100/0/0	100/0/0
SPRT-3	100/0/0	93/7/0	0/100/0	0/100/0	100/0/0	100/0/0	100/0/0	100/0/0

\*The first number denotes the number of accepting the right hypothesis, and the second number denotes the number of rejecting the correct hypothesis. The last one is the number of cases where the SPRT cannot draw decisions based on the given data sets. For example, 100/0/0 means that, out of 100 simulations, 100 cases are correctly assigned to the true hypothesis and there were no misclassification nor undecided cases.

extreme statistics leading the results of SPRT-3 astray. As shown in Figure 3, SPRT-1 again makes the fastest decision among all three SPRTs, and SPRT-2 takes the longest time to select a hypothesis.

### 5.3 Gamma Parent Distribution

Finally, the sequential tests are applied to data sets simulated from a gamma parent distribution. A gamma distribution is often used to describe the  $k$ th occurrence of an event, which constitutes a Poisson process with a mean rate of occurrence,  $\nu$  (Ang and Tang, 1975). The corresponding density function is defined as;

$$f(x) = \frac{\nu(\nu x)^{k-1}}{\Gamma(k)} \exp[-\nu x] \quad x \geq 0 \quad (42)$$

where  $\Gamma(k)$  is the gamma function. Note that the exponential and chi-square distributions are special cases of the gamma distribution, and obtained by setting  $k=1.0$  and  $\nu=0.5$  in Equation (42), respectively. The gamma distribution is skewed to the right for a small value of  $k$ . As the degrees of freedom  $k$  increases the gamma distribution converges to the normal distribution. In this example, the sample data are generated from a gamma distribution with  $k=3$  and  $\nu=0.2$ . This gamma distribution has the skewness value of 1.15 and kurtosis of 5.00, respectively. The associated PDF is plotted in Figure 4.

Hypothesis results similar to the case of the lognormal distribution are obtained in Table 3 and Figure 5. For all three distribution types considered in the examples, SPRT-1 outperforms SPRT-2 and SPRT-3. Humenik and Gross (1990) report a similar observation that the SPRT is

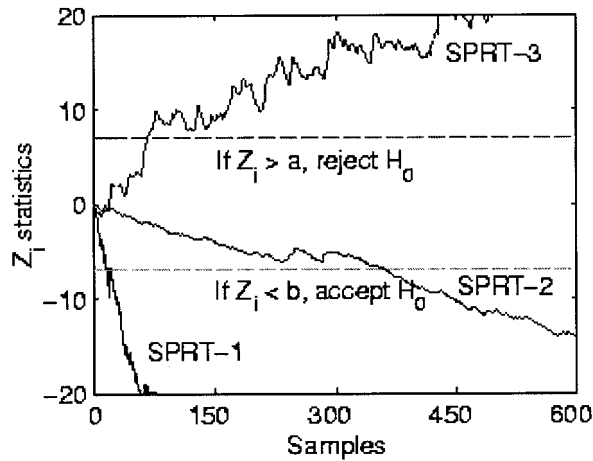


**Figure 5** A typical damage classification result for data sets from a gamma distribution (Correct decision: accepting  $H_0$ ).

robust in the sense that the SPRT works well even if the underlying distribution is not exactly Gaussian. Again, the results of SPRT-3 seem unreliable especially near the lower decision bound. Therefore, the application of SPRTs to the subsequent experimental data is limited to SPRT-1 and SPRT-2.

## 6 Experimental Test

In order to validate the applicability of the proposed technique to structural health monitoring problems, the SPRT analysis combined with time series analysis and extreme value statistics is applied to acceleration time history signals measured from a three-story building model constructed in a laboratory environment. This test structure is built as part of Los Alamos Dynamics Summer School Program (<http://www.lanl.gov/projects/dss>), where upper level undergraduate students and first year graduate students spend 8 weeks at Los Alamos National Laboratory attending lectures and working on several hands-on experiments. Different damage detection approaches are also demonstrated using this test structure (Adams and Farrar, 2002; Worden et al., 2002).

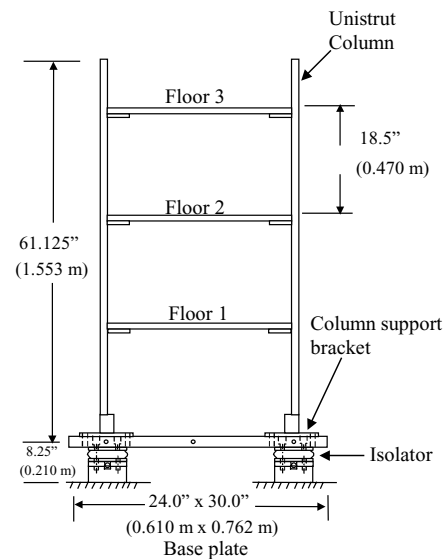


**Figure 6** A three-story frame structure with dimension and damage locations.

### 6.1 Description of a Test Structure

The three-story frame structure model is shown in Figure 6. The structure consists of Unistrut columns and aluminum floor plates. The floors are 1.3 cm-thick (0.5 in.) aluminum plates with two-bolt connections to brackets on the Unistrut. The base is a 3.8 cm-thick (1.5 in.) aluminum plate. Support brackets for the columns are bolted to this

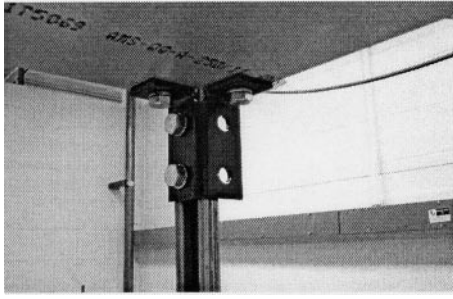


**Figure 7** A bolted joint of the test structure.

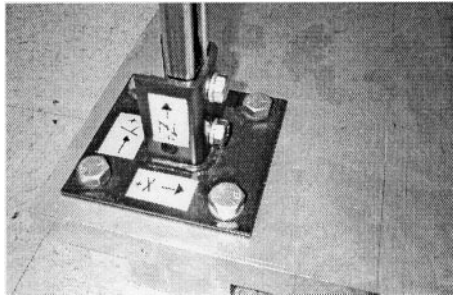


**Figure 8** The connection to the base plate.

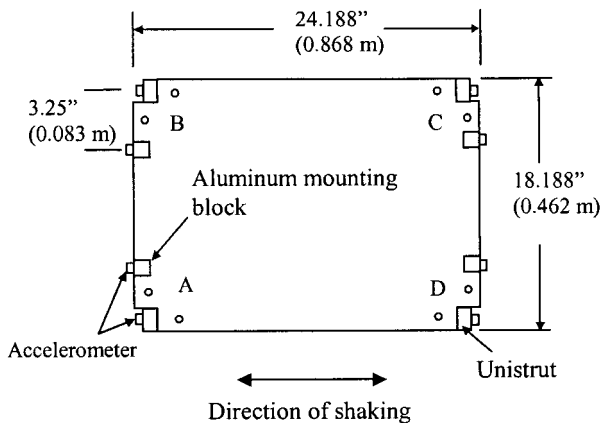


**Figure 9** Floor layout as viewed from above.

plate and hold the Unistrut columns. The details of these joints are shown in Figures 7 and 8. The floor layout from the top of the structure is shown in Figure 9. All bolted connections are tightened to a torque value of 0.7 N m (60 in. lbs) in the undamaged state. Four Firestone air mount isolators, which allow the structure to move freely in horizontal directions, are bolted to the bottom of the base plate. The isolators are inflated to

140 kPa gauge (20 psig) and then adjusted to allow the structure to sit level with the shaker.

The structure is instrumented with 24 piezo-electric single-axis accelerometers, two per joint as shown in Figure 9. The accelerometers are numbered from the corner A to D counterclockwise and from the top floor to the first floor. Accelerometers are mounted on the aluminum blocks that are attached by hot glue to the plates and columns. This configuration allows relative motion between the column and the floor to be monitored. The nominal sensitivity of each accelerometer is 1 V/g. The shaker is coupled to the structure by a 15 cm long (6 in.), 9.5 mm diameter (0.375 in.) stinger connected to a tapped hole at the midheight of the base plate. The shaker is attached at corner D of the base floor (below floor 1), as shown in Figure 6, so that both translational and torsional motions can be excited. The RMS voltage of the shake was fixed at 2 V, and random signals were generated from the shaker. A 2.25 mV/N (10 mV/lb) force transducer is also mounted between the stinger and the base plate. This force transducer is used to measure the input to the base of the structure. A commercial data acquisition system controlled from a laptop PC is used to digitize the accelerometer and force transducer analog signals. The data sets that were analyzed in the feature extraction and statistical modeling portion of the study were the acceleration time histories. Each time signal gathered consisted of 8192 points and was sampled at 1600 Hz.

Two damage cases are investigated in this experiment. The first damage is introduced at the corner A of the first floor (Damage 1) and the second damage is placed at the corner C of the third floor (Damage 2). These two damage locations are shown in Figure 6. For each damage case, four bolts at each joint are loosened until hand tight, allowing relative movement between the floor plate and column. After each damage case, all the bolts were tightened again to the initial torque of 0.7 N m (60 in. lbs). Five time series are measured from the initial undamaged case, and these time series are used for training and constructing the reference database. Five time series are recorded under each damage cases, and additional five time series are obtained after

tightening all bolts to the initial torque values. These time series are used for testing the proposed SPRT procedure. That is, a total of 20 time series are used for this experiment.

## 6.2 Damage Classification Results

Instead of independently analyzing 24 time histories from each accelerometer, the point-by-point difference between time series from the two adjacent accelerometers at individual joint is first computed. Then, the resulting 12 time series corresponding to each joint are used for the AR-ARX modeling. The order  $r$  in the AR model of Equation (2) is set to 25, and the  $p$  and  $q$  orders for the ARX model of Equation (5) are set to 20 and 5, respectively. Satisfactory prediction error, the standard deviation of which is mostly less than 10% of the original signal, is achieved using the AR-ARX model for all the reference signals indicating that the selected AR-ARX model appropriately characterizes the underlying dynamic system of each signal readings.

Next, SPRT-1 and SPRT-2 are applied to the damage-sensitive feature obtained from the AR-ARX modeling, i.e., the residual errors. The Type I & II errors are set to 0.001 as before.

The formulation of the SPRT here is based on the premise that, when a system being monitored undergoes a structural change such as damage, a signal measured under the new structural condition will be significantly different from the signal obtained from the initial undamaged case. Therefore, when a time prediction model is constructed using the baseline undamaged time signal, the prediction error of the newly obtained signal, which is again from a damaged case, will depart from that of the baseline signal. In particular, the prediction error of the new signal is expected to increase. Based on this observation, the sequential hypothesis test for SPRT-1 is cast as follows:

$$H_0 : \sigma \leq \sigma_0, \quad H_1 : \sigma \geq \sigma_1, \quad 0 < \sigma_0 < \sigma_1 \quad (43)$$

In this particular example,  $\sigma_0$  and  $\sigma_1$  are set to 0.40 and 0.42, respectively. Note that the establishment of the  $\sigma_0$  and  $\sigma_1$  values is based on the observation of actual damage cases. That is, changes of the standard deviation are first monitored for at least several damage cases to select the appropriate  $\sigma_0$  and  $\sigma_1$  values. This selection of the  $\sigma_0$  and  $\sigma_1$  values categorizes the proposed method as a supervised learning method. In a

**Table 4** Damage classification results using SPRT-1.

Test Case	Ch1– Ch2	Ch3– Ch4	Ch5– Ch6	Ch7– Ch8	Ch9– Ch10	Ch11– Ch12	Ch13– Ch14	Ch15– Ch16	Ch17– Ch18	Ch19– Ch20	Ch21– Ch22	Ch23– Ch24
Undamaged	0	0	0	0	0	0	0	0	0	0	0	0
	0	0	0	0	0	0	0	0	0	0	0	0
	0	0	0	0	0	0	0	0	0	0	0	0
	0	0	0	0	0	0	0	0	0	0	0	0
	0	0	0	0	0	0	0	0	0	0	0	0
Damage 1	0	0	0	0	0	0	0	0	1	0	0	0
	0	0	0	0	0	0	0	0	1	0	0	0
	0	0	0	0	0	0	0	0	1	0	0	0
	0	0	0	0	0	0	0	0	1	0	0	0
	0	0	0	0	0	0	0	0	1	0	0	0
Damage 2	0	0	0	1	0	0	0	0	0	0	0	0
	0	0	0	1	0	0	0	0	0	0	0	0
	0	0	0	1	0	0	0	0	0	0	0	0
	0	0	0	1	0	0	0	0	0	0	0	0
	0	0	0	1	0	0	0	0	0	0	0	0

• The zero '0' denotes that the null hypothesis is accepted indicating no damage is present at that joint, and the unity '1' denotes that the null hypothesis is rejected and the corresponding joint is damaged. The shaded areas represent the locations of the actually damaged joints, and the hypothesis results in these shaded areas should ideally correspond to 1. The hypothesis results should be zero otherwise.

• For each undamaged and damage cases, five time series are recorded, and the corresponding damage classification results are shown.



**Table 5** Damage classification results using SPRT-2.

Test Case	Ch1– Ch2	Ch3– Ch4	Ch5– Ch6	Ch7– Ch8	Ch9– Ch10	Ch11– Ch12	Ch13– Ch14	Ch15– Ch16	Ch17– Ch18	Ch19– Ch20	Ch21– Ch22	Ch23– Ch24
Undamaged	0	0	0	0	0	0	0	0	0	0	0	0
	0	0	0	0	0	0	0	0	0	0	0	0
	0	0	0	0	0	0	0	0	0	0	0	0
	0	0	0	0	0	0	0	0	0	0	0	0
	0	0	0	0	0	0	0	0	0	0	0	0
Damage 1	0	0	0	0	0	0	0	0	1	0	0	0
	0	0	0	0	0	0	0	0	1	0	0	0
	0	0	0	0	0	0	0	0	1	0	0	0
	0	0	0	0	0	0	0	0	1	0	0	0
	0	0	0	0	0	0	0	0	1	0	0	0
Damage 2	0	0	1	1	0	0	0	0	0	0	0	0
	0	0	0	1	0	0	0	0	0	0	0	0
	0	0	0	1	0	0	0	0	0	0	0	0
	0	0	1	1	0	0	0	0	0	0	0	0
	0	0	1	1	0	0	0	0	0	0	0	0

• The zero '0' denotes that the null hypothesis is accepted indicating no damage is present at that joint, and the unity '1' denotes that the null hypothesis is rejected and the corresponding joint is damaged. The shaded areas represent the locations of the actually damaged joints, and the hypothesis results in these shaded areas should ideally correspond to 1. The hypothesis results should be zero otherwise.

• For each undamaged and damage cases, five time series are recorded, and the corresponding damage classification results are shown.

similar fashion, the sequential hypothesis test for SPRT-2 is cast as follows;

$$H_0 : \sigma_M \leq \sigma_{M,o}, \quad H_1 : \sigma_M \geq \sigma_{M,1}, \quad (44)$$

$$0 < \sigma_{M,o} < \sigma_{M,1}$$

where  $\sigma_{M,0}$  and  $\sigma_{M,1}$  are set to 0.24 and 0.26 based on a similar observation as before.

The results of damage classification using SPRT-1 and SPRT-2 are reported in Tables 4 and 5. In both tables, the zero '0' entity denotes that the null hypothesis is accepted indicating that no damage is present at that joint, and the one '1' entity denotes that the null hypothesis is rejected and the corresponding joint is damaged. The shaded areas in the tables represent the locations of the actually damaged joints, and the hypothesis results in these shaded areas should ideally correspond to one. The hypothesis results should be zero otherwise.

Briefly summarizing the results, SPRT-1 and SPRT-2 demonstrate comparable performances. Both SPRT-1 and SPRT-2 do not show any false-positive indications of damage for all five undamaged cases. For the first damage case (Damage 1), the damaged joints are located at

the corner A on the first floor, and these joints are associated with sensor readings from channels 17 and 18. Using SPRT-1 and SPRT-2, the actual damage location is correctly revealed for all five cases. For the second damage case (Damage 2), where the bolts at the corner C on the third floor are loosened, SPRT-1 indicates that the adjacent joint at the corner D on the same floor is most likely damaged. SPRT-2 also suggests the existence of damage at the same adjacent joint but correctly identifies the actually damaged joint 3 times out of the five examined time series. It should be noted that because the probability distribution of the features used in this specific experiment was inherently close to a Gaussian distribution, there were no significant differences between SPRT-1 and SPRT-2 analyses. In addition, the plot of  $Z$  statistic could have oscillatory behavior. For instance, when the system to be monitored is intact at the beginning, the  $Z$  statistic continues to decrease. Once damage initiates, the  $Z$  statistic starts to increase (moves to the opposite direction) and eventually crosses the upper threshold value indicating damage. Furthermore, the more non-stationary the system response is, the more oscillatory the  $Z$  statistic becomes. However,

because the primary objective of using the SPRT is to identify damage, the user is not concerned with the fluctuation of the  $Z$  statistic. Once the  $Z$  statistic goes across the upper threshold value, inspection or repair of the system need to be performed and the SPRT needs to be reset. However, it would be interesting to introduce some “weighting factor” to the  $Z$  statistic so that the data corresponding to the undamaged case of the structure are not weighed too much before damage occurrence. Otherwise, it would take a longer time for the  $Z$  statistic to response to damage.

## 7 Conclusion

A unique integration of time series analysis, statistical inference, and extreme value theory is provided to address the issue of damage identification. Time series analysis techniques, which are solely based on the measured vibration signals, are first employed to extract damage-sensitive features for damage classification. While there had been increasing interest in the field of structural health monitoring, decisions as to whether a structure is damaged or not tend to be made on the basis of exceeding some heuristic threshold. In this study, the sequential probability ratio test (SPRT) is employed to provide a more principled statistical tool for this decision-making procedure, excluding unnecessary interpretation of the measured data by users. Finally, the performance and robustness of damage classification is improved by incorporating extreme values statistics of the extracted features into the SPRT. The applicability of the SPRT to structural health monitoring is demonstrated using time signals measured from a three-story frame structure tested in a laboratory environment. The framework of the proposed SPRT is well suited for developing a continuous monitoring system, and can be easily implemented on digital signal processing (DSP) chips automating the damage classification process.

## References

Adams, D.R. and Farrar, C.R. (2002). Application of frequency domain ARX features for linear and non-

- linear structural damage identification. *Proceedings of SPIE's 9th Annual International Symposium on Smart Structures and Materials*, San Diego, CA, 17–21 March.
- Ang, A.H.-S. and Tang, W.H. (1975). *Probability concepts in engineering planning and design*, John Wiley & Sons, New York, NY.
- Box, G.E., Jenkins, G.M. and Reinsel, G.C. (1994). *Time series analysis: forecasting and control*, Third Edn., Prentice-Hall, New Jersey.
- Castillo, E. (1987). *Extreme value theory in engineering*, Academic Press, San Diego, CA.
- Doebbling, S.W., Farrar, C.R., Prime, M.B. and Shevitz, D.W. (1998). A review of damage identification methods that examine changes in dynamic properties. *Shock and Vibration Digest*, 30(2), 91–105.
- Embrechts, P., Kluppelberg, C. and Mikosch, T. (1997). *Modeling extremal events*, Springer-Verlag, New York, NY.
- Fisher, R.A. and Tippett, L.H.C. (1928). Limiting forms of the frequency distributions of the largest or smallest members of a sample. *Proceedings of the Cambridge Philosophical Society*, 24, 180–190.
- Galambos, J. (1978). *The asymptotic theory of extreme order statistics*, John Wiley and Sons, New York, NY.
- Ghosh, B.K. (1970). *Sequential tests of statistical hypotheses*, Addison-Wesley, Menlo Park, CA.
- Gross, K.C. and Humenik, K.E. (1991). Sequential probability ratio tests for nuclear plant component surveillance, *Nuclear Technology*, 93, 131–137.
- Gumbel, E.J. (1958). *Statistics of extremes*, Columbia University Press, New York, NY.
- Humenik, K.E. and Gross, K.C. (1990). Sequential probability ratio tests for reactor signal validation and sensor surveillance applications. *Nuclear Science and Engineering*, 105, 383–390.
- Kotz, S. and Nadarajah, S. (2000). *Extreme value distributions: theory and applications*, Imperial College Press, London, UK.
- Ljung, L. (1987). *System identifications: theory for the user*, Prentice Hall, Englewood Cliffs, NJ.
- Sohn, H. and Farrar, C.R. (2001). Damage diagnosis using time series analysis of vibration signals. *Journal of Smart Materials and Structures*, 10, 446–451.
- Sohn, H., Farrar, C.R., Hunter, N.F. and Worden, K. (2001). Structural health monitoring using statistical pattern recognition techniques. *ASME Journal of Dynamic Systems, Measurement and Control: Special Issue on Identification of Mechanical Systems*, 123(4), 706–711.
- Wald, A. (1947). *Sequential Analysis*, John Wiley and Sons, New York, NY.